

Parallel Majorization Minimization with Dynamically Restricted Domains for Nonconvex Optimization: Supplementary Material

Yan Kaganovsky*
Duke University

Ikenna Odinaka*
Duke University

David Carlson
Columbia University

Lawrence Carin
Duke University

Abstract

We provide proofs for the theorems presented in the main paper and additional numerical examples.

1 Proofs of Theorems and Lemmas

1.1 Proof of Lemma 2.1

Proof First, we need to verify that the conditions in (3)–(7) are satisfied. It follows directly from (14) that $\bar{F}(\hat{\theta}; \hat{\theta}) = F(\hat{\theta})$ and $\nabla_{\theta}\bar{F}|_{\theta=\hat{\theta}} = \nabla_{\theta}F|_{\theta=\hat{\theta}}$ so (4)–(5) are satisfied. Also, by construction the entries of D in (15) are non-negative so XDX^T is a positive semi definite matrix and $(\theta - \hat{\theta})^T XDX^T(\theta - \hat{\theta}) \geq 0$, so $\bar{F}(\theta) \geq F$ for any $\theta \in \mathbb{R}^p$, so (3) is satisfied. Note that the majorization domain $\hat{\Omega}_M$ is a (non-empty) convex polyhedron so the domain of the surrogate is convex. Also, $\hat{\theta} \in \text{int}(\hat{\Omega}_M)$ and $\hat{\theta} \in \Omega_F$ by assumption so (6)–(7) are satisfied. Lastly, we check that the function is convex on $\hat{\Omega}_M$. The Hessian of \bar{F} is $\mathcal{H}(\theta) = X\text{Diag}(\{f''_m(\theta^T x_m)\}_{m=1}^M)X^T + XDX^T$. From the definition of D in (15) and (11) it follows that $\mathcal{H}(\theta) \succeq 0$ for $\theta \in \hat{\Omega}_M$, thus proving the convexity of \bar{F} on $\hat{\Omega}_M$. \square

1.2 Proof of Lemma 2.2

Proof Define the line $L(\alpha) := \{\lambda\theta_2 + (1 - \lambda)\theta_1 | \lambda \in (0, \alpha)\}$. Since $\theta_1, \theta_2 \in \Omega_F$ and Ω_F is convex, then $L(1) \subseteq \Omega_F$ and since $\theta_1 \in \text{int}(\Omega_M)$ there exists $\alpha_0 > 0$ such that $\emptyset \neq L(\alpha_0) \subseteq \Omega_M$. For $\alpha_0 \leq 1$, we also have $L(\alpha_0) \subseteq L(1) \subseteq \Omega_F$ and therefore $L(\alpha_0) \subseteq \Omega_F \cap \Omega_M$. Let $\theta^* := \lambda\theta_2 + (1 - \lambda)\theta_1$ with $\lambda \in (0, \alpha_0)$, then $\theta^* \in L(\alpha_0) \subseteq \Omega_F \cap \Omega_M$. Since F is convex we have $F(\theta^*) \leq \lambda F(\theta_2) + (1 - \lambda)F(\theta_1) < F(\theta_1)$, where in the last inequality we used $F(\theta_2) < F(\theta_1)$. \square

Appearing in Proceedings of the 19th International Conference on Artificial Intelligence and Statistics (AISTATS) 2016, Cadiz, Spain. JMLR: W&CP volume 51. Copyright 2016 by the authors. * Indicates equal contributions.

1.3 Proof of Lemma 2.3

Proof Let $g(w) : \mathbb{R} \rightarrow \mathbb{R}$ be a convex function. From Jensen's inequality $g(\sum_k w^k) = g(\sum_k r^k(w^k/r^k)) \leq \sum_k r^k g(w^k/r^k)$ for any $r = [r^1; r^2; \dots; r^K] \in \mathbb{R}^K$ with $1 \leq K \leq p$, s.t. $r \succeq 0$ and $\|r\|_1 = 1$. Now set $g_m(v) = \tilde{f}_m(\hat{\theta}^T x_m + v)$ (recall that \tilde{f} in (16) is globally convex) and rewrite $\tilde{f}_m(\theta^T x_m) = g_m((\theta - \hat{\theta})^T x_m)$ and then apply the above inequality with $w^k = (\theta^k - \hat{\theta}^k)^T x_m^k$ for each m separately which leads to $\tilde{f}_m(\theta^T x_m) \leq \sum_k r_m^k \tilde{f}_m(\hat{\theta}^T x_m + (\theta^k - \hat{\theta}^k)^T x_m^k/r_m^k)$. For each m we choose the r_m^k given in (20) which satisfies the conditions of Jensen's inequality. From (16), (12), and (11) it follows that $\tilde{f}_m(\theta^T x_m) \leq \tilde{f}_m(\hat{\theta}^T x_m) \leq \sum_k r_m^k \tilde{f}_m(\hat{\theta}^T x_m + (\theta^k - \hat{\theta}^k)^T x_m^k/r_m^k)$ for any m and for any $\theta \in \hat{\Omega}_M$. Summing over m we obtain that $F \leq \sum_m \mathcal{S}_m$ with \mathcal{S}_m defined in (19) which proves that (3) holds for $\hat{\Omega}_M$. By using (12) and (16), it is simple to check directly that (4)–(7) are satisfied. \square

1.4 Proof of Lemma 3.2

Proof We have $x^* \in \mathcal{A}(x^*)$ and the constraints as specified by Ω_F in (1) are qualified. Then there exist Lagrange multipliers $\{\eta_i^*\}_{i=1}^I \subset \mathbb{R}$ and $\{\mu_j^*\}_{j=1}^J \subset \mathbb{R}$ such that the following KKT conditions hold

$$\nabla \mathcal{C}(x^*) + \sum_{i=1}^I \eta_i^* \nabla g_i(x^*) + \sum_{j=1}^J \mu_j^* \nabla h_j(x^*) = 0 \quad (\text{A1})$$

$$g_i(x^*) \leq 0, \quad \eta_i^* \geq 0, \quad g_i(x^*)\eta_i^* = 0, \quad \forall i \in [I] \quad (\text{A2})$$

$$h_j(x^*) = 0, \quad \mu_j^* \in \mathbb{R}, \quad \forall j \in [J], \quad (\text{A3})$$

where $[I] = \{1, 2, \dots, I\}$ and $[J] = \{1, 2, \dots, J\}$, and we used (5) so that $\nabla \mathcal{S}(x^*) = \nabla \mathcal{C}(x^*)$. Equations (A1)–(A3) are exactly the KKT conditions for the program in (1) which are satisfied by $(x^*, \{\eta_i^*\}_{i=1}^I, \{\mu_j^*\}_{j=1}^J)$, and therefore x^* is a stationary point of (1). \square

1.5 Proof of Theorem 3.3

Proof $\Omega_F \subset \mathbb{R}^p$ is assumed closed and bounded, and it is therefore compact. $\theta^{(t)} \in \Omega_F$ so $\theta^{(t)}$ lies in a

compact set for all t and (1) in Theorem 3.1 is satisfied. Let Γ be the set of all generalized fixed points of \mathcal{A} and let $\phi = \mathcal{C}$. Property 2(b) in Theorem 3.1 follows directly from the descent property in (9). To obtain 2(a) in Theorem 3.1 (the case of $\theta^{(t)} \notin \Gamma$), note that it is equivalent to stating that if there exists $\theta^{(t+1)} \in \mathcal{A}(\theta^{(t)})$ such that $\mathcal{C}(\theta^{(t+1)}) = \mathcal{C}(\theta^{(t)})$ then $\theta^{(t+1)} \in \Gamma$, i.e., $\theta^{(t+1)}$ is a generalized fixed point, which follows by definition. To prove the closeness of \mathcal{A} we break it into two maps $\mathcal{A}(\theta^{(t)}) = \mathcal{A}_2(\mathcal{A}_1(\theta^{(t)}))$ where \mathcal{A}_1 is the map obtained by the minimization of the surrogate and \mathcal{A}_2 is the projection onto $\Omega_M^{(t)}$. The closeness of \mathcal{A}_1 follows from the existence of the solution to $\{\theta^* = \arg \min_{\theta} \mathcal{S}(\theta; \theta^{(t)}) : \theta \in \Omega_F\}$, the continuity of \mathcal{S} and proposition 7 in (Gunawardana and Byrne, 2005). The closeness of \mathcal{A}_2 follows from the continuity of the one-to-one mapping in (18). The composition of two closed mappings is also closed, thus 2(c) in Theorem 3.1 is satisfied. Since Ω_F is bounded and closed, by the Bolzano-Weierstrass theorem there exists a convergent subsequence of $\{\theta^{(t)}\}_{t=1}^{\infty}$ in Ω_F . By Theorem 3.1, any such sequence will converge to a generalized fixed point, which is also a stationary point of (1) by Lemma 3.2. \square

2 Sigmoid-Loss SVM

Figure 1 shows a comparison between the loss functions considered in this work

$$0-1: \quad f(z) = (-\text{sign}(z) + 1)/2, \quad (\text{A4})$$

$$\text{hinge:} \quad f(z) = \max(0, 1 - z), \quad (\text{A5})$$

$$\text{logistic:} \quad f(z) = \log(1 + \exp(-z)), \quad (\text{A6})$$

$$\text{sigmoid:} \quad f(z) = 1 - \tanh(z). \quad (\text{A7})$$

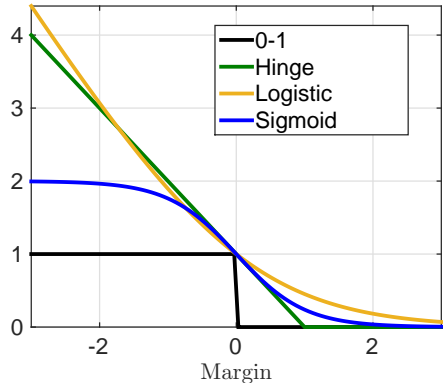


Figure 1: A comparison between the 0-1, logistic, Hinge, and Sigmoid loss functions.

3 Example for Choosing the Majorization Domain

To illustrate the majorization-minimization procedure proposed in the paper, a simple 1D example is shown in Fig. 2, where the blue curve is the original objective, the green curve is the global surrogate when $[a, b] = (-\infty, \infty)$, and the red curve is the local surrogate when $[a, b]$ are chosen according to Algorithm 4.1 and Algorithm 4.2 (“shallow region” case). It can be seen in Fig. 2 that using the local surrogate with lower curvature leads to taking a larger step than when using a global surrogate. Note that at the iteration shown, each surrogate leads to taking a step from the expansion point (marked by an asterisk) to the minimum of the surrogate (marked by circles). It should be noted however, that the minimum for the high-dimensional problem in (2) does not necessarily occur at the minimum points of f_m . Also note that all surrogates are convex but neither of them are quadratic.

4 Additional Details Regarding the Numerical Experiments

Experiments performed on the MNIST dataset utilize all the available examples for digit “3” (6131 for training, and 1010 for testing) and for digit “5” (5421 for training, and 892 for testing). We used the standardized features for MNIST. For the 20Newsgroups dataset, we also used all available examples for newsgroup 1 (480 for training, and 318 for testing) and for newsgroup 20 (376 for training, and 251 for testing). The feature vectors from the 20 Newsgroups dataset were transformed using the transformation $\log(1 + x)$, which led to an improvement in performance. For the TB dataset we split the data into 80% training and 20% testing examples, which amounts to 260 training and 70 testing examples for HIV negative, and 133 training and 28 test examples for HIV positive. We used the raw features of the TB dataset to keep their interpretability (gene expression) which is important for understanding which genes contribute to a good prediction of HIV (feature selection). This also provides a good example for the *scale-invariance* of the proposed PMM method. In order to determine the regularization constant λ we use cross-validation with a 80% – 20% split of the training set into training and validation sets.

All algorithms were run till one of the following stopping criteria was met: (1) the relative change in the objective between two consecutive iterations was less than 10^{-6} ; (2) the magnitude of the gradient was less than 10^{-8} ; (3) the relative change in the norm of θ between two consecutive iterations was less than 10^{-2} .

Table 1: Classification accuracy (%) on **test** set using Logistic regression. LIBLIN uses an L1 penalty and the rest of the methods use a nonconvex log-penalty. For the latter, 10 different random initializations were used and the mean and standard deviation are presented. GD=Gradient Descent, RProp=RMSProp, AGrad=AdaGrad, PMM=Parallel Majorization-Minimization, DRD=Dynamically Restricted Domain.

Method	MNIST	20 News	TB
LIBLIN	96.69	79.61	89.69
LBFGS	96.13 \pm 0.11	76.2 \pm 1.06	88.45 \pm 1.34
CG	96.4 \pm 0.13	77.93 \pm 0.85	85.57 \pm 2.06
GD	95.6 \pm 0.68	77.21 \pm 3	87.63 \pm 0.73
PSCA	89.54 \pm 0	68.7 \pm 0.36	46.19 \pm 0.46
RProp	96.34 \pm 0.11	83.18 \pm 0.63	55.26 \pm 25.05
AGrad	95.17 \pm 0.08	81.3 \pm 0.34	54.84 \pm 24.67
PMM	96.27 \pm 0	75.89 \pm 0.32	90.72 \pm 0
PMM-DRD	96.49 \pm 0.17	76.68 \pm 0.17	90.72 \pm 0

References

A. Gunawardana, and W. Byrne (2005). Convergence Theorems for Generalized Alternating Minimization Procedures. *Journal of Machine Learning Research* 6:2049–2073.

5 Additional Results

Table 1 shows the classification accuracy (%) on **test** set using Logistic regression.

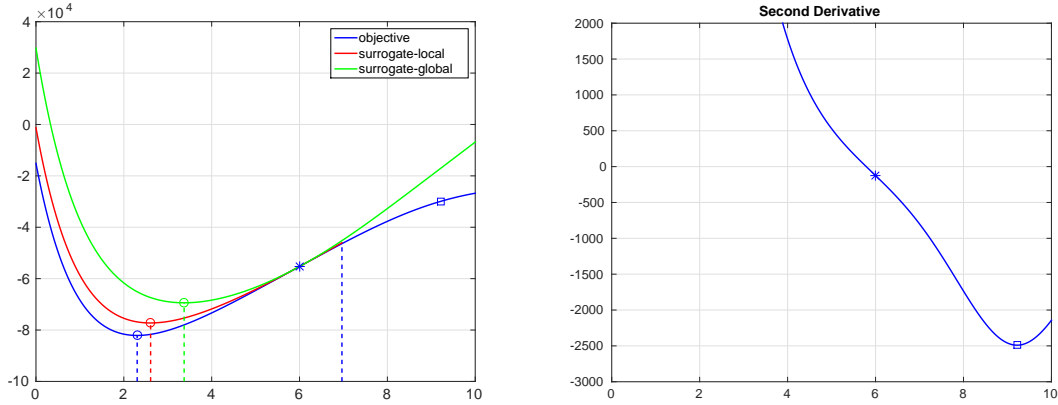


Figure 2: Top: an example of the proposed local (red curve) and global (green curve) surrogate for a 1D function (blue curve) given by $f(x) = I \exp(-x) + r - y \log(I \exp(-x) + r)$ with $I = 10^5$, $y = 10^4$, $r = 10$. Bottom: second derivative of f . The expansion point (marked by an asterisk) is located at a “shallow region”. The majorization domain for the local surrogate is $[a, b] = (-\infty, 7]$, which is computed by Algorithm 4.1 and Algorithm 4.2. The right boundary b is chosen between the point of minimum curvature (marked by a square) and the expansion point. Here we chose $\alpha = 0.5$ and $\beta = 0.3$ for the parameters of Algorithm 4.1. The convex extension of the local surrogate beyond b is not shown.